

New small molecule inhibitors of histone methyl transferase DOT1L with a nitrile as a non-traditional replacement for heavy halogen atoms

Sophie S. Spurr,^a Elliott D. Bayle,^a Wenyu Yu,^b Fengling Li,^b Wolfram Tempel,^b Masoud Vedadi,^b Matthieu Shapira,^b and Paul V. Fish^{a,*}

^a UCL School of Pharmacy, University College London, 29-39 Brunswick Square, London WC1N 1AX, UK

^b Structural Genomics Consortium, University of Toronto, 101 College Street, MaRS Centre, South Tower, Toronto M5S 1L7, Canada

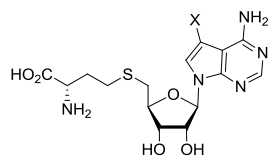
Key words: protein methyltransferase, DOT1L inhibitors, toyocamycin, bioisostere, cyano-deaza-SAH.

*Address correspondence to PVF at Alzheimer's Research UK UCL Drug Discovery Institute, The Cruciform Building, University College London, Gower Street, London WC1N 1E 6BT, UK; Tel: +44 (0)20 7679 6971; e.mail: p.fish@ucl.ac.uk.

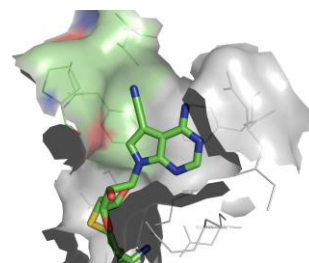
Graphical Abstract

New small molecule inhibitors of histone methyl transferase DOT1L with a nitrile as a non-traditional replacement for heavy halogen atoms

Sophie S. Spurr, Elliott D. Bayle, Wenyu Yu, Fengling Li, Wolfram Tempel, Masoud Vedadi, Matthieu Shapira, Paul V. Fish



Br-SAH X = Br: DOT1L IC₅₀ = 77 nM
CN-SAH (**19**) X = CN: DOT1L IC₅₀ = 26 nM



Crystal structure of CN-SAH (**19**) in DOT1L (PDB 5JUW, 2.3 Å)

Abstract

A number of new nucleoside derivatives are disclosed as inhibitors of DOT1L activity. SARs established that DOT1L inhibition could be achieved through incorporation of polar groups and small heterocycles at the 5-position (**5**, **6**, **12**) or by the application of alternative nitrogenous bases (**18**). Based on these results, CN-SAH (**19**) was identified as a potent and selective inhibitor of DOT1L activity where the polar 5-nitrile group was shown by crystallography to bind in the hydrophobic pocket of DOT1L. In addition, we show that a polar nitrile group can be used as a non-traditional replacement for heavy halogen atoms.

DOT1L is a protein methyltransferase known to methylate lysine 79 of histone 3 (H3K79), an epigenetic mark associated with transcriptionally active genes.¹ Chromosomal translocations recurrent in leukemia result in oncogenic fusions between MLL and a variety of genes, such as AF4 or AF9, that recruit DOT1L to aberrant genomic loci, and transcriptional activation of leukemic genes.² Small molecule inhibitors of DOT1L activity can reverse the oncogenic reprogramming of MLL-rearranged leukemia,^{3,4} and the first-in-class DOT1L inhibitor pinometostat (EPZ-5676; Epizyme) has progressed to Phase I clinical trials for the treatment of pediatric patients with relapsed/refractory leukemias bearing a rearrangement of the MLL gene.⁵

Most current DOT1L inhibitors, such as EPZ004777 and EPZ-5676, compete with the methyl donating cofactor S-adenosyl-L-methionine (SAM). These SAM analogues lock a conformationally dynamic loop of the enzyme into an inactive state.^{6,7} In a variation on this theme, recently reported structurally novel inhibitors of DOT1L also antagonize the formation of an enzymatically active state, but only partially occupy the cofactor site.^{8,9} Selective inhibition of DOT1L can also be achieved by functionalizing the adenosine ring of S-adenosyl-L-homocysteine (SAH), the reaction product of SAM (Figure 1). Bromo-deaza-SAH (Br-SAH) is a potent and selective inhibitor of DOT1L activity with a bromine atom that occupies a hydrophobic cavity specific to DOT1L, but this compound is inactive in cell based systems, probably due to poor cell penetration.¹⁰ Modification of EPZ004777 by introduction of a bromine atom on the adenosine ring gave SGC0946 and both compounds selectively kill human cord blood cells transformed with an MLL-AF9 fusion oncogene.⁷ However, the poor pharmacokinetic properties of EPZ004777 precluded conventional dosing methods for efficacy studies in a mouse xenograft model of MLL.³ Nonclinical in vivo pharmacokinetics of EPZ-5676 in mouse, rat and dog showed moderate to high clearance and low oral bioavailability,¹¹ and so EPZ-5676 was administered by continuous intravenous infusion in the Phase I clinical trial.^{5,11}

As part of our research efforts to discover new inhibitors of DOT1L activity with improved pharmacokinetic properties, we adopted a strategy to identify novel functional groups that would favourably exploit the hydrophobic cavity adjacent to the adenine binding site of SAH in DOT1L. In addition, we wished to avoid the use of heavy halogen atoms as they confer higher lipophilicity to drug molecules which tends to be detrimental to drug-like properties. In this Letter, we disclose cyano-deaza-SAH (**19**, CN-SAH) as a potent and selective inhibitor of DOT1L activity that incorporates a polar nitrile group which binds in this hydrophobic pocket.

Previously, a screen of a library of 3120 kinase inhibitors had identified 5-iodotubercidin (**3**, 5-ITC) as an inhibitor of DOT1L activity (IC₅₀ 18.2 μM) which was subsequently optimised to Br-SAH (IC₅₀ 0.077 μM).¹⁰

We adopted a related approach where the tubercidin template (**2**) was investigated as a model system with the objective of transferring preferred structure-activity-relationships (SARs) into more relevant templates for potential use as biochemical and structural tools, chemical probes with cell activity, and ultimately to chemical leads suitable for convenient dosing in preclinical in vivo efficacy studies.

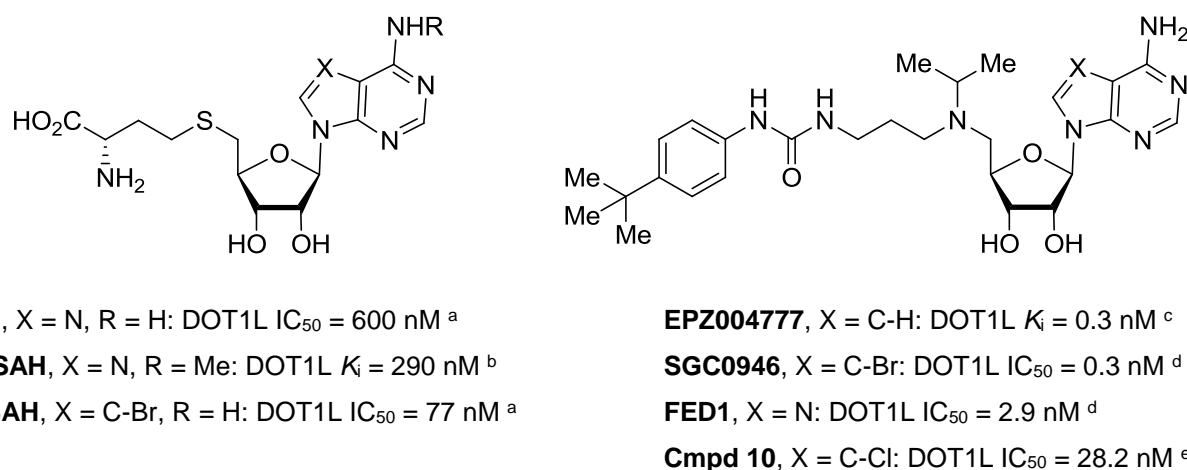


Figure 1. Structures of DOT1L inhibitors. ^a Yu et al. [10]; ^b Yao et al. [12]; ^c Daigle et al. [3]; Basavapathruni et al. [6]; ^d Yu et al. [7]; ^e Yi et al. [13].

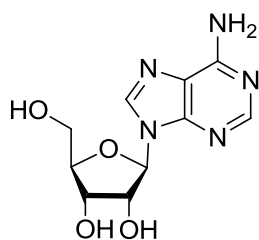
The nucleoside target compounds were either purchased from commercial sources (**1-6**, **13-15**) or prepared using short synthetic sequences (**7-12**, **16-18**) as described in detail in the Supplementary Material. The DOT1L inhibitory activity of target compounds **1-19** (Table 1) was evaluated by the assay conditions as reported by Yu et al. with minor modifications (see: Supplementary Material).¹⁰

The SARs were initially focused on exploring the substitution at the 5-position (tubercidin numbering used throughout), which presents this substituent towards the hydrophobic pocket adjacent to the adenine binding site of SAH in DOT1L (PDB code 3QOX); this interaction has been successfully exploited by 5-ITC (**3**: X = I)(PDB code 3UPW) and Br-SA(H) (PDB code 3SX0).¹⁰ Adenosine (**1**) and tubercidin (**2**: X = H) were very weakly active with 20-40 % inhibition at 200 μM respectively which supported the benefits of a group at this 5-position. Toyocamycin (**5**: X = CN), a bacterial metabolite with a diverse range of activities,¹⁴ showed promising activity as did sangivamycin (**6**: X = CONH₂). These results were somewhat

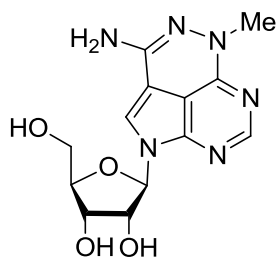
unexpected as replacing a lipophilic iodine atom ($\pi +1.12$) with a polar nitrile ($\pi -0.57$) or primary carboxamide group ($\pi -1.49$) is not a traditional bioisostere transformation.^{15, 16} The aromatic chloride to nitrile transformation has been reviewed by Jones et al.^{16b} whereas there are far fewer reports of the corresponding aromatic iodide to nitrile substitution in medicinal chemistry design.^{17, 18} However, in the context of this work, these results demonstrated the hydrophobic pocket could accommodate both lipophilic and polar groups assuming the binding mode was retained (*vide infra*).

Further SARs with synthetic analogues showed 5-fluorine **7**, 5-phenyl **10** or 5-benzyl **11** derivatives were similar in activity to tubercidin. The 5-ethyne **8** was equipotent to toyocamycin (**5**) although extending the alkyne further with a 5-(2-cyclopropylethyne) group **9** lost activity (<20 % I @ 200 μ M). The use of an oxazole **12** as a surrogate for the *p*-carboxamide of **6** showed that a small heterocyclic group could be accommodated with retention of activity.

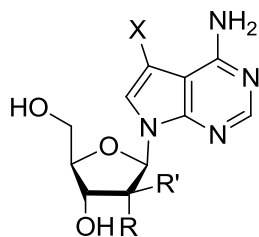
Limited SAR of the ribose showed that the 2'-hydroxy was important for binding (**13** v **3**: X = I) as **13** was inactive (<20 % I @ 200 μ M). The addition of a 2' β -Me (**14** v **2**: X = H) failed to improve activity as **14** was also inactive (<20 % I @ 200 μ M) albeit with only the inferior 5-H substituent. Modification of the nitrogenous base proved to be more successful. Although 3-deazaadenosine (**15**) was inactive (< 20 % I @ 200 μ M) confirming the preference of the N atom at this position (**15** v **1**), modification of the base at the 6-position by substitution of the 6-CH for a 6-N demonstrated that the pyrazolo [3,4-*d*]pyrimidine could be of comparable potency to the pyrrolo[2,3-*d*]pyrimidine (**18** v **3**: X = I *cf.* **17** v **2**: X = H). DOT1L inhibitory activity was again superior when combined with the 5-iodo substituent as **18** was one of the most potent inhibitors from this model system.



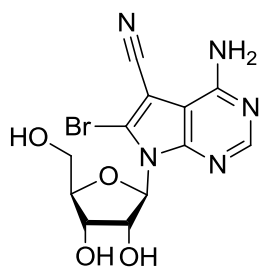
1 adenosine



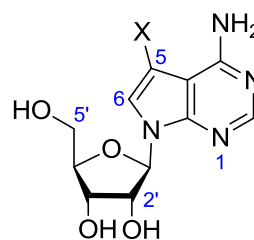
4 triciribine



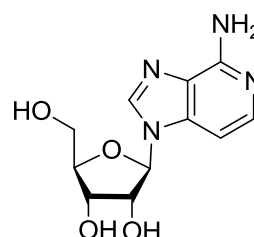
13 X = I; R = R' = H
14 X = H; R = OH; R' = Me



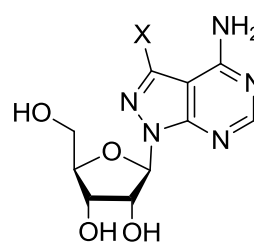
16



X =
2 H tubercidin
3 I 5-iodotubercidin
5 CN toyocamycin
6 CONH₂ sangivamycin
7 F
8 C≡CH
9 C≡CcPr
10 Ph
11 4-PMB
12 2-oxazole



15 3-dezaadenosine



17 X = H
18 X = I

Compound	DOT1L	
	% inhibition at 200 or 250 μM ^a	IC ₅₀ (μM) ^a
1	26 \pm 4 % I @ 200 μM	
2	41 \pm 4 % I @ 200 μM	
3		7 \pm 2 ^c
4	< 20 % I @ 200 μM	
5		44 \pm 10
6		26 \pm 7
7	ca. 52 \pm 5 % I @ 200 μM ^b	ca. 200 ^b
8		41 \pm 12
9	< 20 % I @ 200 μM	
10	44 \pm 5 % I @ 200 μM	
11	42 \pm 1 % I @ 250 μM	
12		43 \pm 8
13	< 20 % I @ 200 μM	
14	< 20 % I @ 200 μM	
15	< 20 % I @ 200 μM	
16	ca. 50 \pm 4 % I @ 200 μM ^b	ca. 200 ^b
17	< 20 % I @ 200 μM	
18		22 \pm 2
19		0.026 \pm 0.005

Table 1. ^a Assay conditions: DOT1L (0.2 nM), [³H]-SAM (0.7 μM), chicken nucleosome (0.1 μM), buffer: 20 mM Tris pH8, 5 mM DTT, 10 mM MgCl₂, 0.01% Triton X-100. In general, IC₅₀s were determined side by side from 11-point dose response curves with test concentrations from 0.20 to 200 μM , except **11** (0.50 to 500 μM) and **19** (0.01 to 10 μM). Experiments were performed in triplicate with data presented as the mean \pm SD. ^b Incomplete concentration-inhibition S-curve. ^c Data are presented for comparison in a common assay format. Literature values for 5-ITC (**3**): DOT1L IC₅₀ = 18.2 μM . See reference [10].

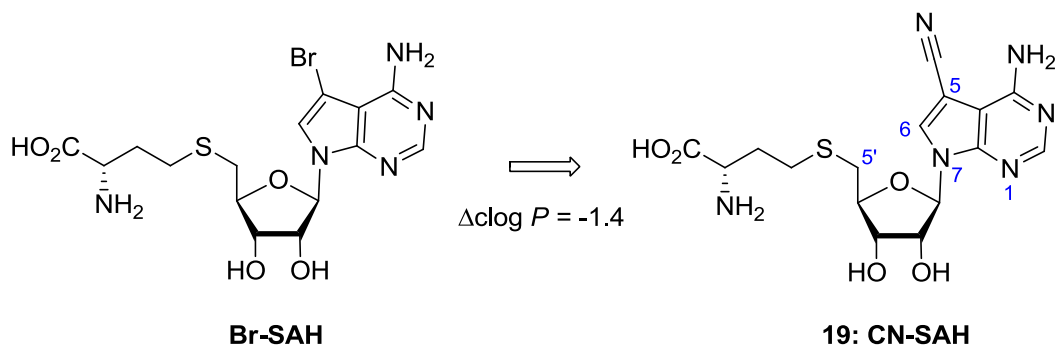
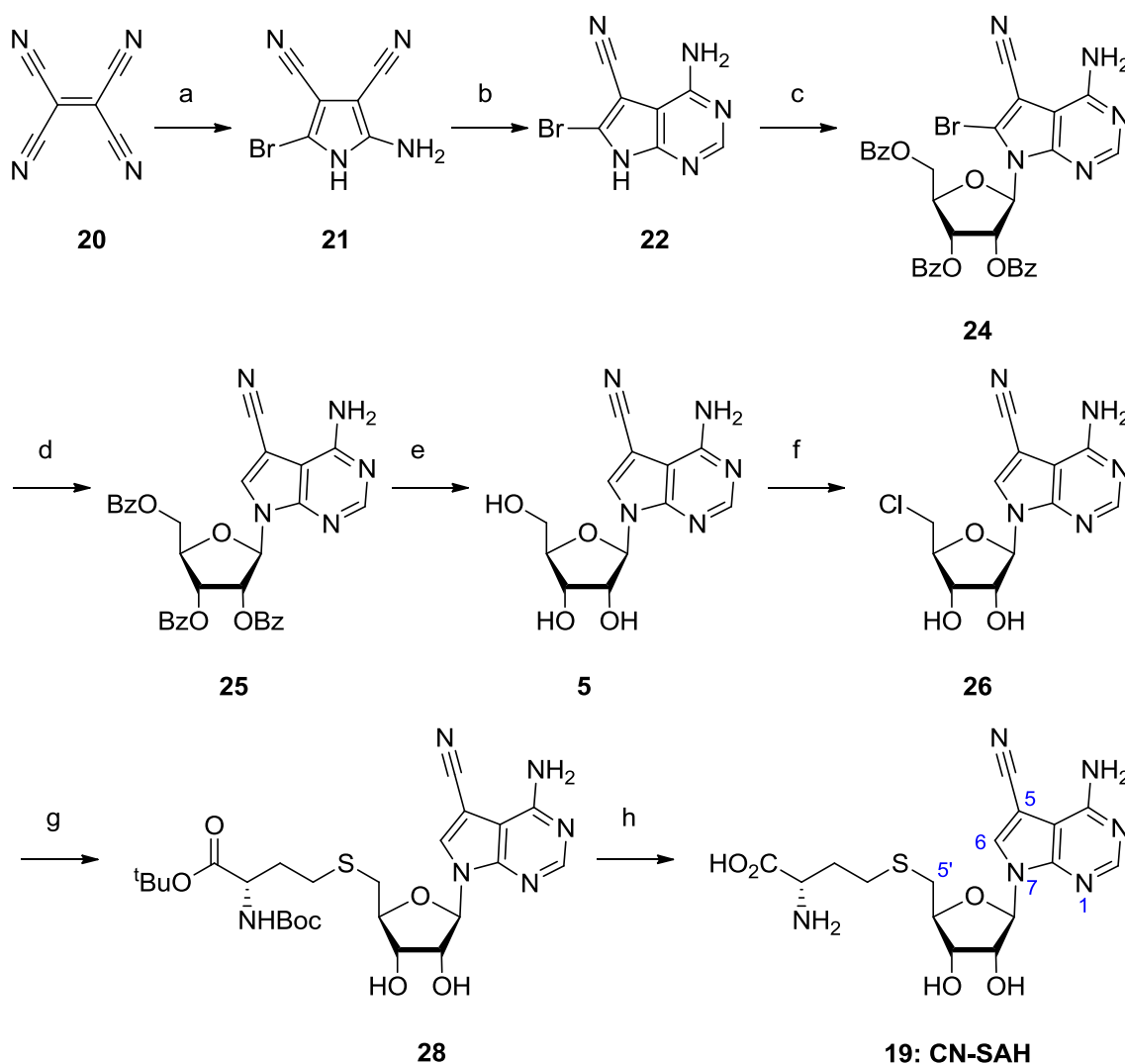


Figure 2. Design of CN-SAH (**19**).

Based on these results, we selected toyocamycin (**5**) with the 5-nitrile as the starting point for the design of the biochemical tool cyano-deaza-SAH (**19**, CN-SAH) as proof-of-principle to deliver potent and selective inhibitors of DOT1L that incorporate polar groups that bind in the hydrophobic pocket (Figure 2). We anticipated these polar groups could then be applied to identify new DOT1L chemical probes and would improve the ‘drug-like’ properties of this template by significantly lowering the overall lipophilicity.¹⁹



Scheme 1. Synthesis of CN-SAH (**19**). Reagents and conditions: (a) 33% HBr in AcOH, acetone, EtOAc, 0 °C - rt, 3 h, 60 %; (b) formamidine acetate, 2-ethoxyethanol, reflux, 24 h, 36 %; (c) (i) HMDS, TMSCl, reflux 18 h, then (ii) evaporate and add MeCN, then (iii) β -D-Ribofuranose-1-acetate-2,3,5-tribenzoate (**23**), TMSOTf, reflux, 3 h, 49 %; (d) ammonium formate, 5 mol% Pd/C, EtOH, reflux, 3 h, 65 %; (e) 7 M NH₃ in MeOH, 0 °C - rt, 12 h, 60 %; (f) SOCl₂, DMPU, 0 °C, 5 h, 50 %; (g) (i) KI, K₂CO₃, DMF, rt, 5 min, then (ii) *t*-Butyl Boc-L-homocysteinate (**27**), 80 °C, 5 h, 75 %; (h) 4 M HCl in dioxane, 0 °C, 7 h, 82 %.

The synthesis of CN-SAH (**19**) is described in Scheme 1.²⁰ This 8-step sequence follows published procedures to related compounds with minor modifications to improve yields/selectivities or the substitution of highly toxic reagents for safer alternatives.^{10, 21} The preferential N7 glycosylation of pyrrolo[2,3-d]pyrimidine **22** with furanose **23** was achieved with 1,1,1,3,3,3-hexamethyldisilazane (HMDS) as described recently by Kim *et al.* to give **24**.²² Reduction of the C6-Br by catalytic transfer hydrogenation gave **25** and then deprotection of the benzoates afforded toyocamycin (**5**).²¹ Conversion of the 5'-OH to the corresponding 5'-chloride **26** activated the 5' position of the sugar ready for the introduction of the homocysteine moiety. This followed the procedure of Yu *et al.*¹⁰ except that *t*-butyl Boc-L-homocysteinate (**27**) was used which greatly improved the efficiency of the reactions even with the additional step to simultaneously deprotect the homocysteine acid and amine groups.

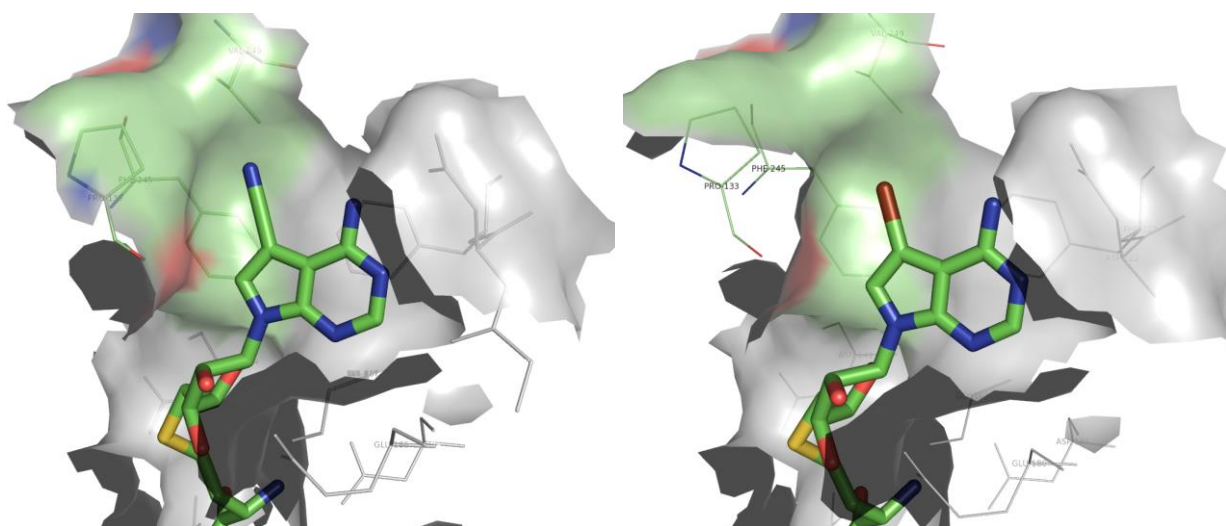


Figure 3. Co-crystal structures of **CN-SAH (19)** (PDB code 5JUW, left) and **Br-SAH** (PDB code 3SX0, right) in DOT1L. Images generated with PyMOL.

CN-SAH (**19**) was shown to be a potent inhibitor of DOT1L with an IC_{50} value of 26 nM (Table 1). To establish the binding mode, we solved the structure of CN-SAH in complex with DOT1L (2.3 Å, PDB code 5JUW). As expected, the structure is nearly identical to DOT1L in complex with SAM (PDB code 1NW3) and Br-SAH (PDB code 3SX0). The activation loop of DOT1L is folded on the cofactor mimetic, in a conformationally active state. The nitrogen atom of the 5-nitrile of CN-SAH occupies the hydrophobic pocket composed of V249, L224, P133, and F245 as previously exploited by the bromine of Br-SAH.

MTase (h)	CN-SAH (19) IC ₅₀ (μM) ^a	Br-SAH IC ₅₀ (μM) ^b	SAH IC ₅₀ (μM)
DOT1L	0.013	0.077	0.22
DNMT1	0.15	1.9	0.20
PRMT3	0.87	2.3	2.0
PRMT5	2.4	2.3	0.20
G9a	99	no inhibition	4.1
SETD7	no inhibition	no inhibition	47
SUV39H2	no inhibition	no inhibition	22
EZH2	no inhibition	no inhibition	65

Table 2. Inhibition of DOT1L activity and MTase selectivity profiles of CN-SAH (**19**), Br-SAH and SAH.

^a Screened at Eurofins Cerep (France). In general, IC₅₀s were determined from 8-point dose response curves (test concentrations: 30 nM to 100 μM) except DOT1L which required a lower dynamic range (0.1 nM to 1 μM). Data is the mean of two replicates. SAH was used as a reference compound throughout and data are presented for comparison in a common assay format. See: Supplementary Material.

^b Reference [10].

CN-SAH (**19**) was confirmed to be a potent inhibitor of DOT1L (IC₅₀ = 13 nM) by independent evaluation (Table 2 and Supplementary Material). In addition, CN-SAH was 17-times more potent than SAH against DOT1L which, like the bromine atom of Br-SAH, shows the nitrile group of CN-SAH better exploits the hydrophobic pocket of DOT1L. CN-SAH was then screened against a panel of representative protein lysine (PKMT), protein arginine (PRMT) and DNA (DNMT) methyltransferases to establish the selectivity profile (Table 2). CN-SAH was inactive at concentrations up to 100 μM against the PKMTs EZH2 (as part of PRC2 complex), SUV39H2 and SETD7 although there was very weak activity for G9a. CN-SAH showed inhibitory activity for both PRMT3 and the PRMT5 complex but with acceptable selectivity at 66- and 180-fold respectively. The selectivity of CN-SAH over these PRMTs is modestly improved when compared to BrSAH (both 30-fold) which reflects improved affinity for DOT1L rather than weaker activity for the PRMTs. CN-SAH was shown to be an inhibitor of DNMT1 with only 11-fold selectivity and would need to be improved.

In summary, we have designed and evaluated a number of new nucleoside derivatives as inhibitors of DOT1L activity. SARs established that DOT1L inhibition could be achieved through incorporation of polar groups and small heterocycles at the 5-position (**5**, **6**, **12**) or by the application of alternative nitrogenous bases (**18**). Based on these results, CN-SAH (**19**) was identified as a potent and selective inhibitor of DOT1L activity where the polar 5-nitrile group was shown by crystallography to bind in the hydrophobic pocket of

DOT1L. The next phase of these studies will be to develop CN-SAH into a chemical probe that is active in cell-based models and with good oral activity in rodent models of disease.

Acknowledgments

We are grateful to the UCL Drug Discovery PhD Studentship Programme (to S.S.S.) for financial support. HRMS were recorded at the EPSRC UK National Mass Spectrometry Facility (NMSF) at Swansea University, UK. We also acknowledge the contribution of Prima Patel and Adil Butt for their assistance, John R. Walker for suggestions toward crystallographic model refinement and Peter J. Brown for his support.

The SGC is a registered charity (number 1097737) that receives funds from AbbVie, Bayer Pharma AG, Boehringer Ingelheim, Canada Foundation for Innovation, Eshelman Institute for Innovation, Genome Canada through Ontario Genomics Institute, Innovative Medicines Initiative (EU/EFPIA) [ULTRA-DD grant no. 115766], Janssen, Merck & Co., Novartis Pharma AG, Ontario Ministry of Economic Development and Innovation, Pfizer, São Paulo Research Foundation-FAPESP, Takeda, and the Wellcome Trust. Results shown in this report are derived from work performed at Argonne National Laboratory, Structural Biology Center at the Advanced Photon Source. Argonne is operated by UChicago Argonne, LLC, for the U.S. Department of Energy, Office of Biological and Environmental Research under contract DE-AC02-06CH11357.

Supplementary Material

Sources of compounds **1-6**, **13 – 15** and synthetic schemes for compounds **7 – 12**, **16-18**. ¹H and ¹³C NMR data for **CN-SAH (19)**. Materials and methods for the DOT1L IC₅₀ determinations. Crystal structure data and model statistics.

References and notes

1. For a review, see: (a) A. T. Nguyen, Y. Zhang. *Genes Dev.* **2011**, *25*, 1345. While DOT1L is believed to be the main enzyme to write this epigenetic mark associated with transcriptionally active genes, an isoform of WHSC1 was recently reported to also methylate H3K79; see, (b) J. Woo Park, K. B. Kim, J. Y. Kim, Y. C. Chae, O. S. Jeong, S. B. Seo, *Sci. Rep.* **2015**, *5*, 12485.

2. K. M. Bernt, N. Zhu, A. U. Sinha, S. Vempati, J. Faber, A. V. Krivtsov, Z. Feng, N. Punt, A. Daigle, L. Bullinger, R. M. Pollock, V. M. Richon, A. L. Kung, S. A. Armstrong. *Cancer Cell* **2011**, *20*, 66.
3. S. R. Daigle, E. J. Olhava, C. A. Therkelsen, C. R. Majer, C. J. Sneeringer, J. Song, L. D. Johnston, M. P. Scott, J. J. Smith, Y. H. Xiao, L. Jin, K. W. Kuntz, R. Chesworth, M. P. Moyer, K. M. Bernt, J. C. Tseng, A. L. Kung, S. A. Armstrong, R. A. Copeland, V. M. Richon, R. M. Pollock. *Cancer Cell* **2011**, *20*, 53.
4. S. R. Daigle, E. J. Olhava, C. A. Therkelsen, A. Basavapathruni, L. Jin, P. A. Boriack-Sjodin, C. J. Allain, C. R. Klaus, A. Raimondi, M. Porter Scott, N. J. Waters, R. Chesworth, M. P. Moyer, R. A. Copeland, V. M. Richon, R. M. Pollock. *Blood* **2013**, *122*, 1017.
5. Phase 1 Dose Escalation and Expanded Cohort Study of EPZ-5676 in the Treatment of Pediatric Patients With Relapsed/Refractory Leukemias Bearing a Rearrangement of the MLL Gene.
ClinicalTrials.gov identifier: NCT02141828
6. A. Basavapathruni, L. Jin, S. R. Daigle, C. R. A. Majer, C. A. Therkelsen, T. J. Wigle, K. W. Kuntz, R. Chesworth, R. M. Pollock, M. P. Scott, M. P. Moyer, V. M. Richon, R. A. Copeland, E. J. Olhava. *Chem. Biol. Drug Des.* **2012**, *80*, 971.
7. W. Y. Yu, E. J. Chory, A. K. Wernimont, W. Tempel, A. Scopton, A. Federation, J. J. Marineau, J. Qi, D. Barsyte-Lovejoy, J. N. Yi, R. Marcellus, R. E. Jacob, J. R. Engen, C. Griffin, A. Aman, E. Wienholds, F. L. Li, J. Pineda, G. Estiu, T. Shatseva, T. Hajian, R. Al-awar, J. E. Dick, M. Vedadi, P. J. Brown, C. H. Arrowsmith, J. E. Bradner, M. Schapira. *Nat. Commun.* **2012**, *3*, 1218.
8. C. Chen, H. Zhu, F. Stauffer, G. Caravatti, S. Vollmer, R. Machauer, P. Holzer, H. Mobitz, C. Scheufler, M. Klumpp, R. Tiedt, K. S. Beyer, K. Calkins, D. Guthy, M. Kiffe, J. Zhang, C. Gaul. *ACS Med. Chem. Lett.* **2016**, *XX*, XXXX. DOI: [10.1021/acsmchemlett.6b00167](https://doi.org/10.1021/acsmchemlett.6b00167)
9. C. Scheufler, H. Möbitz, C. Gaul, C. Ragot, C. Be, C. Fernández, K. S. Beyer, R. Tiedt, F. Stauffer. *ACS Med. Chem. Lett.* **2016**, *XX*, XXXX. DOI: [10.1021/acsmchemlett.6b00168](https://doi.org/10.1021/acsmchemlett.6b00168)
10. W. Yu, D. Smil, F. Li, W. Tempel, O. Fedorov, K. Nguyen, Y. Bolshan, R. Al-Awar, S. Knapp, C. Arrowsmith, M. Vedadi, P. Brown, M. Schapira. *Bioorg. Med. Chem.*, **2013**, *21*, 1787.

11. Nonclinical pharmacokinetics and metabolism of EPZ-5676: (a) A. Basavapathruni, E. J. Olhava, S. R. Daigle, C. A. Therkelsen, L. Jin, P. A. Boriack-Sjodin, C. J. Allain, C. R. Klaus, A. Raimondi, M. Porter Scott, A. Dovletoglou, V. M. Richon, Roy M. Pollock, R. A. Copeland, M. P. Moyer, R. Chesworth, P. G. Pearson, N. J. Waters. *Biopharm. Drug Dispos.* **2014**, *35*, 237. However, the plasma clearance of EPZ-5676 was recently shown to be markedly lower in human compared to preclinical species, see: (b) S. A. Smith, S. Gagnon, N. J. Waters. *Xenobiotica* **2016**, *XX*, XXXX. DOI:10.3109/00498254.2016.1173265
12. Y. Yao, P. Chen, J. Diao, G. Cheng, L. Deng, J. L. Anglin, B. V. V. Prasad, Y. Song. *J. Am. Chem. Soc.* **2012**, *134*, 17834.
13. J. S. Yi, A. J. Federation, J. Qi, S. Dhe-Paganon, M. Hadler, X. Xu, R. St Pierre, A. C. Varca, L. Wu, J. J. Marineau, W. B. Smith, A. Souza, E. J. Chory, S. A. Armstrong, J. E. Bradner. *ACS Chem. Biol.* **2015**, *10*, 667.
14. R. L. Tolman, R. K. Robons, L. B. Townsend. *J. Am. Chem. Soc.* **1969**, *91*, 2102.
15. Hydrophobic fragmental constants (π) are used as a measure of lipophilicity.
16. For reviews on bioisosteres, see: (a) N. A. Meanwell. *J. Med. Chem.* **2011**, *54*, 2529; (b) L. Jones, N. Summerhill, N. Swain, J. Mills. *Med. Chem. Commun.* **2010**, *1*, 309.
17. A. S. Bell, S. F. Campbell, D. S. Morris, D. A. Roberts, M. H. Stefaniak. *J. Med. Chem.* **1989**, *32*, 1552.
18. For a review of aromatic iodide to nitrile substitution in synthetic chemistry, see: G. P. Ellis, T. M. Romney-Alexander. *Chem. Rev.* **1987**, *87*, 779.
19. For a review on the benefits of reducing lipophilicity of drug candidates, see: P. D. Leeson, B. Springthorpe. *Nat. Rev. Drug Disc.* **2007**, *6*, 881.
20. (S)-2-amino-4-(((2S,3S,4R,5R)-5-(4-amino-5-cyano-7H-pyrrolo[2,3-d]pyrimidin-7-yl)-3,4-dihydroxytetrahydrofuran-2-yl)methyl)thio)butanoic acid dihydrochloride salt was prepared as an off-white amorphous solid (45 mg) (**19: CN-SAH**): m.p. 130-5 °C (dec.); $[\alpha]_D^{25} +16$ (c 0.5, MeOH); IR ν_{\max} (neat) 2922.36 (br), 2232.60 (s), 1665.52 (s), 1518.04 (s), 1427.84 (s), 1047.29 (s) cm^{-1} ; ^1H NMR (500 MHz, CD_3OD) δ : 8.51 (1H, s, 2/6-CH); 8.48 (1H, s, 2/6-CH); 6.28 (1H, d, $J= 4.4$ Hz, 1'-CH); 4.52 (1H,

t, $J=4.6$ Hz, 2'-CH); 4.28 - 4.23 (2H, m, 3'-CH, 4'-CH); 4.15 (1H, t, $J=6.1$ Hz, Cys- α -CH); 3.07 - 2.99 (m, 2H, 5'-CH₂); 2.81 (2H, t, $J=7.4$ Hz, Cys- γ -CH₂); 2.32 - 2.25 (1H, m, Cys- β -CH); 2.20 - 2.13 (1H, m, Cys- β -CH); ¹³C NMR (125 MHz, CD₃OD) δ : 171.4 (C=O), 152.5, 149.7, 145.8, 135.7, 113.9 (CN), 103.0, 90.7 (C1'), 88.7, 85.6 (C4'), 76.0 (C2'), 73.8 (C3'), 52.7 (Cys- α -CH), 35.0 (C5'), 31.6 (Cys- β -CH₂), 29.0 (Cys- γ -CH₂); LCMS m/z : 409.2 ([M+H]⁺; 92.5 % pure; RT 0.85 min); HRMS (m/z HNEP) for C₁₆H₂₁N₆O₅S [M+H]⁺ calc. 409.1289, observed 409.1284.

21. P. Leonard, S. A. Ingale, P. Ding, X. Ming, F. Seela. *Nucleosides Nucleotides Nucleic Acids* **2009**, *28*, 678.
22. Y. Kim, S. Kwon, I. Bae and B. Kim. *Tetrahedron Lett.* **2013**, *54*, 5484.